Some Consequences of Intense Electromagnetic Wave Injection into Space Plasmas

By

William J. Burke[1], Elena Villalon[2], Paul L. Rothwell[1],

and Michael Silevitch[2]

I Introduction

The past decade has been marked by an increasing interest in performing active experiments in space. These experiments involve the artificial injections of beams, chemicals, or waves into the space environment. Properly diagnosed, these experiments can be used to validate our understanding of plasma processes, in the absence of wall effects. Sometimes they even lead to practical results. For example, the plasma-beam device on SCATHA became the prototype of an automatic device now available for controlling spacecraft charging at geostationary orbit.

In this paper we discuss the future possibility of actively testing our current understanding of how energetic particles may be accelerated in space or dumped from the radiation belts using intense electromagnetic energy from ground based antennas. The ground source of radiation is merely a convenience. A space station source for radiation that does not have to pass through the atmosphere and lower ionosphere, is an attractive alternative. The text is divided into two main sections addressing the possibilities of (1) accelerating electrons to fill selected flux tubes above the Kennel-Petscheck limit for stably trapped fluxes and (2) using an Alfven maser to cause rapid depletion of energetic protons or electrons from the radiation belts. Particle acceleration by electrostatic waves have received a great deal of attention over the last few years (Wong et al., 1981; Katsouleas and Dawson, 1983). However, much less is known about acceleration using electromagnetic waves. The work described herein is still in evolution. We only justify its presentation at this symposium based on the novelty of the ideas in the context of space plasma physics and the excitement they have generated among several groups as major new directions for research in the remaining years of this century.

1. Air Force Geophysics Laboratory, Hanscom AFB, MA 01731

2. Center for Electromagnetic Research,
Northeastern University, Boston, MA 02115

II Electron Acceleration by Electromagnetic Waves

One of the first things we were mistaught in undergraduate physics is that electromagnetic (em) waves can't accelerate charged particles. If the particle gains energy in the first half cycle, it loses it in the second half. Teachers are, of course, clever people who want graduate students. So they hold off discussing gyroresonance, in which case, all bets are off. The resonance condition is:

$$(1) \qquad \omega - k_z v_z - n \Omega_o / \gamma = 0$$

Here ω is the frequency of the driving wave, k_z the component of the wave vector along the zero order magnetic field $\underline{B}_o = B_o \hat{z}$, v_z the particle's component of velocity along $\underline{B}_o$ and n is an integer representing an harmonic of the gyrofrequency $\Omega_o = q B_o/m$, γ is the relativistic correction $(1 - v^2/c^2)^{-1/2}$, q is the charge, and m the rest mass of the electron.

Before going into a detailed mathematical analysis it is obvious that there are going to be problems accelerating cold ionospheric electrons to high energies. Higher than first gyroharmonics will have Bessel function multipliers where the argument of the Bessel function is the perpendicular component of the wave vector and the gyroradius. For cold electrons with small gyroradii, all but the zero index Bessel function terms will be small. The second concern can be understood by considering the motion of a charged particle in a circularly polarized wave. Roberts and Buchsbaum (1964) have shown that with an electron in gyroresonance according to eq.(1) and $\underline{v}_\perp$ initially antiparallel to the wave electric field $\underline{E}$ and perpendicular to the wave magnetic field $\underline{B}$, two effects combine to drive it away from resonance. As the electric field accelerates the electron, γ increases, changing the gyrofrequency. The magnetic component of the wave changes v_z and thus, the Doppler shift term. It is only in the case of the index of refraction $n = ck/\omega = 1$ that unrestricted acceleration occurs. In all other cases the electron goes through cycles gaining and losing kinetic energy.

Recently, the SAIC group (Menyuk et al. 1986) has devised a conceptually simple way to understand acceleration by em waves as a stochastic process. In terms of the relativistic **moments** p_z and $p_\perp$, eq.(1) can be rewritten as

$$p_\perp^2 = (n^2 - 1) p_z^2 + 2 n_z p_z mc (n \Omega_o/\omega) + [(n \Omega_o/\omega)^2 - 1] mc^2$$

Depending on the phase velocity of the waves, equation (2) represents a family of ellipses ($n_z = ck_z/\omega < 1$), hyperbolae ($n_z > 1$) and parabolae ($n_z = 1$) in a $p_\perp$, p_z phase space. The zero order Hamiltonian can also be written in the form

$$(2) \qquad H_o/mc^2 = [1 + (p_z/mc)^2 + (p_\perp/mc)^2]^{1/2} - (p_z/mc)(\omega/ck_z)$$

Thus, in $p_\perp$, p_z space constant Hamiltonian surfaces represent families of hyperbolae ($n_z < 1$) ellipses ($n_z > 1$) and parabolae ($n_z = 1$). Hamiltonian surfaces have open topologies for indices of refraction $n_z \leq 1$. The case $n_z = 1$ in which resonance and Hamiltonian surfaces are overlying parabolae is that of unlimited acceleration studied by Roberts and Buschbaum (1964).

In the case of small amplitude waves the intersections of resonance and Hamiltonian surfaces in $p_\perp$, p_z space are very sharp. As the amplitudes of the waves grow so too do the widths of resonance. For sufficiently large amplitudes, resonance widths may extend down to low kinetic energies allowing cold electrons to be stochastically accelerated to relativistic energies.

It should be pointed out that although this model heuristically explains the main conceptual reasons for stochastic acceleration to occur, its validity extends only to small angles θ between $\underline{k}$ and $\underline{B}_o$. At large angles, it is not clear that the zero-order Hamiltonian topologies described above will still hold.

Over the past several months we have developed a rigorous extension of the analytical model of Roberts and Buchsbaum by letting $\underline{k} = k_x \hat{x} + k_z \hat{z}$ assume an arbitrary angle to $\underline{B}_o$. We begin with the Lorentz equation.

$$(3) \qquad \frac{d\underline{p}}{dt} = q \left[\underline{E} + \underline{v} \times (\underline{B}_o + \underline{B}) \right]$$

The relativistic momentum and Hamiltonian are given by $\underline{p} = m \gamma \underline{v}$ and $H = mc^2 \gamma$, respectively. The magnetic field of the wave $\underline{B}$ is related to the electric $\underline{E}$ through Maxwell's equation $\underline{B} = (\underline{c}/\omega)\underline{k} \times \underline{E}$. The time rate of change of the Hamiltonian is

$$(4) \qquad \dot{H} = q \, \underline{E} \cdot \underline{v} = qc^2 \, \underline{E} \cdot \underline{p}/H$$

If we define $E_x = E_1 \cos \phi$, $E_y = - E_2 \sin \phi$ and $E_z = - E_3 \cos \phi$, where $\phi = k_x x + k_z z - \omega t$ then equation (4) may be rewritten in the form

$$(5) \qquad \frac{\dot{H} H}{c^2 \omega} = \frac{qE_1}{\omega} p_x \cos \phi - \frac{qE_2}{\omega} p_y \sin \phi - \frac{qE_3}{\omega} p_z \cos \phi$$

The Lorentz force equation can also be rewritten as

$$(6)\quad \dot{p}_x + p_y \left[\Omega + \frac{qE_2}{m\gamma} \frac{k_x}{\omega} \sin\phi \right] = \frac{qE_1}{\omega} (\omega - K_z \dot{z}) \cos\phi$$

$$(7)\quad \dot{p}_y - p_x \left[\Omega + \frac{qE_2}{m\gamma} \frac{k_x}{\omega} \sin\phi \right] = -\frac{qE_2}{\omega} (\omega - k_z \dot{z}) \sin\phi$$

$$(8)\quad \dot{p}_z - \frac{K_z}{\omega} \dot{H} + \frac{E_3}{E_1} (\dot{p}_x + \Omega p_y) = 0$$

where $K_z = k_z (1 + E_3 k_x / E_1 k_z)$. Equations (5-8) are exact. Our first simplification is to assume $E_2 k_x / \omega = B_z << B_o$, then eqs. (6-8) may be combined to give

$$(9)\quad \frac{4\dot{H}H}{c^2 \omega} = \frac{q}{\omega} (E_1 + E_2) \left[\int_o^t Q' \cos(\sigma + \phi - \sigma' + \phi') dt' + \right.$$

$$\left. + \int_o^t R' \cos (\sigma + \phi - \sigma' - \phi') dt' - 2p_\perp \sin (\sigma + \phi + \alpha) \right]$$

$$+ \frac{q}{\omega} (E_1 - E_2) \left[\int_o^t Q' \cos (\phi - \sigma + \sigma' - \phi') dt' \right.$$

$$\left. + \int_o^t R' \cos(\phi - \sigma + \phi' + \sigma') dt' + 2p_\perp \sin (\phi - \sigma - \alpha) \right]$$

$$- \frac{q}{\omega} E_3 \left\{ 4 \left(p_{zo} + \frac{K_z}{\omega} (H - H_o) \right) \cos\phi \right.$$

$$\left. - \frac{E_3}{E_1} \int_o^t (Q' + R') \left[\cos(\phi + \phi') + \cos (\phi - \phi') \right] dt' \right\}$$

where $\sigma(t) = \int_o^t \Omega(t') dt'$, $\tan \alpha = -(p_{xo}/p_{yo})$,

(the subscript o refers to the initial conditions at $t = 0$), and

$$Q = \frac{qE_1}{\omega} (\omega - K_z \dot{z}) - \frac{qE_2}{\omega} (\omega - k_z \dot{z})$$

$$R = \frac{qE_1}{\omega} (\omega - K_z \dot{z}) + \frac{qE_2}{\omega} (\omega - k_z \dot{z})$$

Primed and unprimed quantities are evaluated at times t' and t, respectively. We note that accelarations represented in Eq. (9) are related to terms multiplying electric fields in right-hand ($E_1 + E_2$), left-hand ($E_1 - E_2$) and parallel E_3 modes.

Our next simplification is to substitute for x and $\dot{z}$ in eq.(9) the zero order solutions (in the electric field amplitude) of eqs. (6-8). That is, we take $x = \rho \cos(\sigma + \alpha)$ where $\rho = v_\perp / \Omega$ is the electron gyroradius and

$$(10) \qquad p_z = \left[p_{zo} + \frac{K_z}{\omega} (H - H_o) \right] .$$

We note that eq.(10) reduces to eq.(2) by taking $K_z = k_z$, which is only valid for small angles between $\underline{k}$ and $\underline{B}_o$. In fact, Figure 1 shows that Hamiltonians with open (hyperbolic or parabolic) topologies in p_z, $p_\perp$ space at small angles between $\underline{k}$ and $\underline{B}_o$ become closed (elliptical) as the angle increases. **The practical implication is that cases of potentially infinite acceleration with $k \approx k_z$ become restricted to finite values at other directions of wave propagation.**

By taking $x = \rho \cos(\sigma + \alpha)$ and expanding terms with $\sin k_x x$ and $\cos k_x x$ in series of Bessel functions, eq. (9) becomes

$$(11) \qquad \frac{4\dot{H}H}{c^2 \omega} = \sum_n T_n$$

$$T_n = \frac{q}{\omega} (E_1 + E_2) J_{n-1} (k_x \rho) \left\{ \sum_m \int_o^t \left[Q' J'_{m+1} \cos(n\theta + m\theta' + \psi + \psi') + R' J'_{m-1} \cos(n\theta - m\theta' + \psi - \psi') \right] dt' + 2p_\perp \cos(n\theta + \Psi) \right\}$$

$$+ \frac{q}{\omega} (E_1 - E_2) J_{n+1} (k_x \rho) \left\{ \sum_m \int_o^t \left[Q' J'_{m+1} \cos(n\theta - m\theta' + \psi - \psi') + R' J'_{m-1} \cos(n\theta + m\theta' + \psi + \psi') \right] dt' + 2p_\perp \cos(n\theta + \psi) \right\}$$

$$- \frac{qE_3}{\omega} J_n (k_x \rho) \left\{ 4 \left(p_{zo} + \frac{K_z}{\omega} (H - H_o) \right) \cos(n\theta + \psi) - \frac{E_3}{E_1} \sum_m \int_o^t (Q' + R') J'_m \left[\cos(n\theta + m\theta' + \psi + \psi') + \cos(n\theta - m\theta' + \psi - \psi') \right] dt' \right\}$$

where $\theta = \int_o^t \Omega(t')\, dt' + \alpha + \pi/2$, $J'_\nu \equiv J_\nu (k_x \rho')$, $(\nu = m, m \pm 1)$
and $\psi = k_z z - \omega t$.

After averaging over the fast (gyroperiod) time dependencies and a good deal of tedious algebra, we obtain that, for each n, the particle energy obeys the following differential equation:

$$(12) \qquad (U + 1)^2 \left(\frac{1}{\omega} \frac{dU}{dt} \right)^2 + V_n (U) = 0$$

where $U = (H - H_o)/H_o$ and

$$V_n(U) = \frac{d_1^2}{4} U^2 \left(U + 2 r_n/d_1 \right)^2 - \psi(o)\sin\phi_n \; d_1 U \left(U + 2r_n/d_1 \right)$$

$$+ \frac{\Sigma_1 - \Sigma_2}{2} \left\{ \left(\Sigma_2 d_1 - \Sigma_1 h_1 \right) \left(G_{n+1}(U) + F_{n+1}(U) \right) + \left(\Sigma_2 d_2 - \Sigma_1 h_2 \right) F_{n+1}(U) \right\}$$

$$- \frac{\Sigma_1 + \Sigma_2}{2} \left\{ \left(\Sigma_1 h_1 + \Sigma_2 d_1 \right) \left(G_{n-1}(U) + F_{n-1}(U) \right) + \left(\Sigma_1 h_2 + \Sigma_2 d_2 \right) F_{n-1}(U) \right\}$$

$$- \Sigma_3^2 \left\{ h_1 \left(G_n(U) + F_n(U) \right) + h_2 F_n(U) \right\} - \left(\psi(O)\cos\phi_n \right)^2$$

where $\Sigma_i = -(q E_i/\omega)\, c/H_o \quad (i=1,2,3), \qquad d_1 = 1 - K_z k_z c^2/\omega^2$

$d_2 = K_z k_z c^2/\omega^2 - k_z \dot{z}_o/\omega, \qquad h_1 = 1 + K_z/k_z\,(d_1 - 1)$

$r_n = 1 - k_z \dot{z}_o/\omega - n\Omega_o/\omega, \qquad h_2 = K_z/k_z\; d_2$

$\psi(0) = v_{\perp o}/2c \left[-(\Sigma_1 + \Sigma_2) J_{n-1}(k_x \rho_o) + (\Sigma_2 - \Sigma_1) J_{n+1}(k_x \rho_o) \right] + v_{zo}/c \; \Sigma_3 J_n(k_x \rho_o),$

$\phi_n = n(\alpha + \frac{\pi}{2}) + k_z z_o$

and $G_\nu(U) = \int_o^U J_\nu^2 \left[k_x \rho(U') \right] U' \, dU'$

$F_\nu(U) = \int_o^U J_\nu^2 \left[k_x \rho(U') \right] dU', \quad (\nu = n, n \pm 1).$

Eq.(12) is in the form of the equations of a harmonic oscillator. Under the limit $\theta = 0$, Eq. (12) becomes the equation derived by Robert and Buchsbaum (1964). The limits of the particles excursion in energy for a given resonance n and electric field E can be found by setting the potentials $V_n(U) = 0$. At wave amplitudes where the range of potentials for different harmonics overlap, we have the onset of stochasticity.

At the present time we have just begun to explore the numerical solutions of equation (12). In Figure 2, we show some of our preliminary results. We assume that $\omega_{pe}/\Omega_o = 0.3$, the electric field amplitude is such that $\Sigma 1 = 0.1$, and the wave frequency is $\omega = 1.8\,\Omega_o$. We consider only the second cyclotron harmonic since this is the closest to satisfying the resonance condition, eq.(1), for initially cold electrons. The components of the wave electric field and the refractive index η are calculated from the cold plasma dispersion relation for electromagnetic waves at any arbitrary angle θ to B_o. It turns out that η is always smaller than, but very close to 1 ($\eta \simeq 0.97$). The maximum allowed

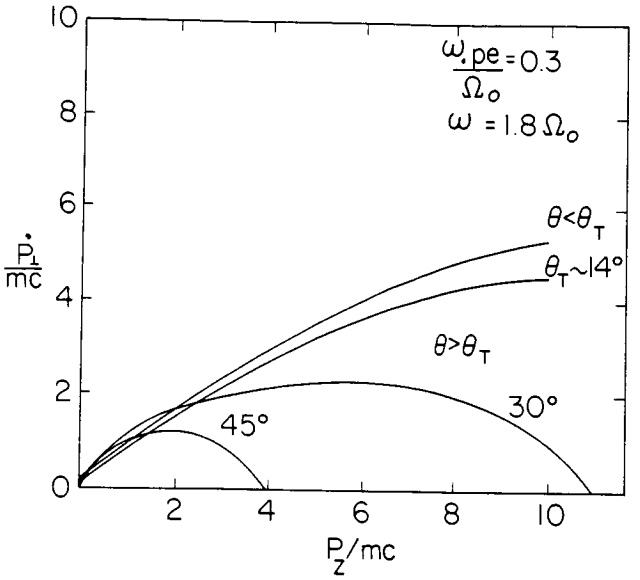

Fig. 1. Surfaces of zero order Hamiltonians with different propagation angles to magnetic field.

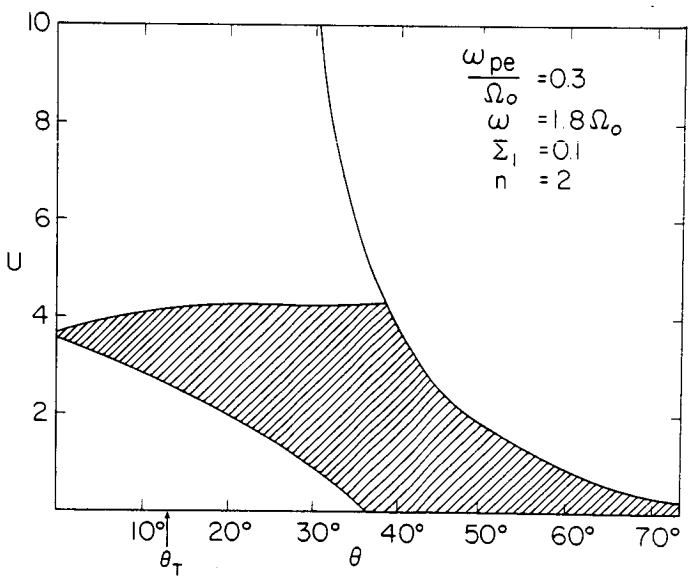

Fig. 2. Range of allowed electron energy gain (shaded) as a function of wave propagation angle to magnetic field. The solid line represents maximum energy excursion for elliptical topologies.

energy gain, as given by the zero order Hamiltonian topologies, is represented by the solid lines . The shaded region represents the actual energy gain as obtained by requiring V_n (U) $\leq$ 0. We see that for $\theta \simeq 35^o$, initially cold electrons can be accelerated to very high energies. In fact, for cold electrons we find that U = γ - 1 and that the particle can gain as much as 2.5 Mev. As θ decreases more initial kinetic energy is required for any acceleration to take place. For large θ , the elliptical hamiltonian topologies severely restrict the energy gain.

III The Alfven Maser

Active control of energetic particle fluxes in the radiation belts has maintained a continuing interest in both the United States and the Soviet Union. Electron dumping experiments concluded by the Stanford University and Lockheed groups using VLF transmissions are well known (Inan et al. 1982, Imhof et al. 1983). Perhaps less known is a theoretical paper by Trakthengerts (1983) entitled "Alfven Masers" in which he proposes a theoretical scheme for dumping both electrons and protons from the belts. The basic idea is to use RF energy to heat the ionosphere at the foot of a flux tube to raise the height integrated conductivity. The conductivity is then modulated at VLF or ELF frequencies which modulates the reflection of waves that cause pitch angle diffusion in the equatorial plane. The artifically enhanced conductivity of the ionosphere thus maintains high wave energy densities in the associated flux tube, thereby producing a masing effect.

In addition to external ionospheric perturbations particle precipitation also raises ionospheric conductivity. The masing of the VLF waves causes further precipitation which, in principle, results in an explosive instability. The purpose of this section is to establish the basic equations and to present the results of a preliminary computer simulation.

The fundamental equations derived by Trakhtengerts (1983) are based on quasilinear theory and relate only to the weak diffusion regime. It is useful to use a similar set of equations derived by Schulz (1974) based on phenomenological arguments that includes strong pitch angle diffusion. The key variables are N, the number of trapped particles per unit area on a flux tube and ε the wave intensity averaged over the flux tube. In this we assume that ε is directly proportioned to the pitch angle diffusion coefficient. The time rate of change for N is

$$(13) \quad \frac{dN}{dt} \quad \frac{-A\ \varepsilon\ N}{1 + \varepsilon\ \tau} \quad + S.$$

where the first term represents losses due to pitch angle scattering with A a constant and S represents particle source terms in the magnetospheric equatorial plane. τ is a parameter that characterizes lifetimes against strong pitch angle diffusion. The time rate of change of ε is given by

$$(14) \quad \frac{d\ \varepsilon}{dt} = \frac{\left(2\ \gamma\ {}^*N/N^* \right)}{1 + \varepsilon\tau}\ \varepsilon + \frac{Vg\ \varepsilon}{LR_e} \ln R + W$$

The first term represents wave growth near the equatorial plane, the second term gives the wave losses in and through the ionosphere and the third accounts for any wave energy sources. The terms γ^* and N^* are used to denote the weak diffusion growth rate and column density of a flux tube at the Kennel and Petschek (1966) limit for stably trapped particles. In the second term, v_g/LR_e approximates bounce frequency of waves where v_g is the group velocity of the wave LR_e the approximate length of a flux tube; R is the reflection coefficient of the ionosphere. Since $R < 1$ the second term is always negative. The $(1 + \varepsilon \tau)$ term empirically lowers growth rate due to the pitch angle distribution becoming more isotropic under strong diffusion conditions.

In our present study we have examined numerical solutions of equations (13) and (14) using non-equilibrium initial conditions. The first case is represented by Figure 3 in which we started initial wave energy densities which are a factor of 3 (top panel) and 0.1 (bottom panel) above the Kennel-Petschek limit. In both cases we ignored associated enhancements in ionospheric coupling that lead to increased reflectivity. We see that the wave energy density quickly damps to the Kennel-Petschek equilibrium represented by the solid line.

In the second level of simulation the wave energy density is initially set at a factor of three above the Kennel-Petschek equilibrium value but includes a coupling factor to the ionosphere ζ. We find that for values of $\zeta \geq 10\%$ the oscillations become spike-like. The top panel of Figure 4 represents the normalized wave energy density for $\zeta = 10\%$ after the waves have evolved into periodic spikes. The middle and bottom panels of Figure 4 represent the normalized energetic particle density (cm^{-2}) contained on a flux tube and the normalized height integrated density of the ionosphere. Attention is directed to the phase relationship between the maxima of the three curves. The maximum, energetic particle flux leads the wave term and goes through the Kennel-Petschek value as the wave growth changes from positive to negative.

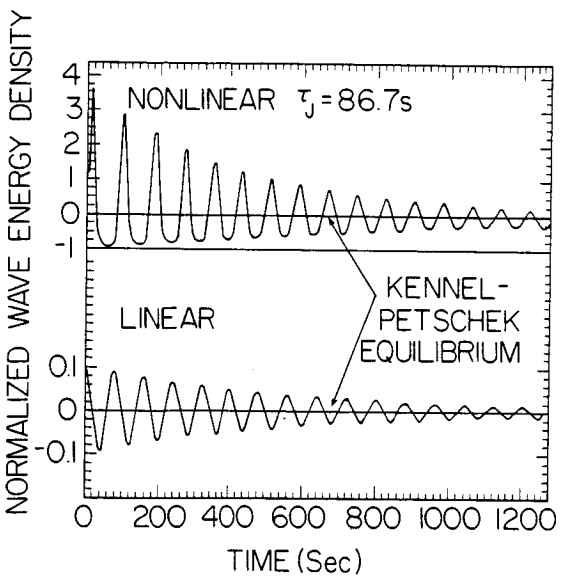

Fig. 3. Example of wave energy densities initially set at factors of 3.0 and 0.1 above Kennel Petschek equilibrium value.

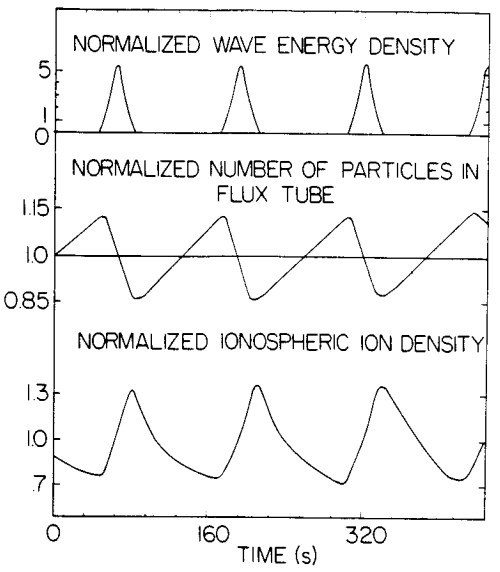

Fig. 4. Example of spike-like wave structures as well as energetic particle losses and ionospheric density changes with magnetosphere-ionosphere coupling.

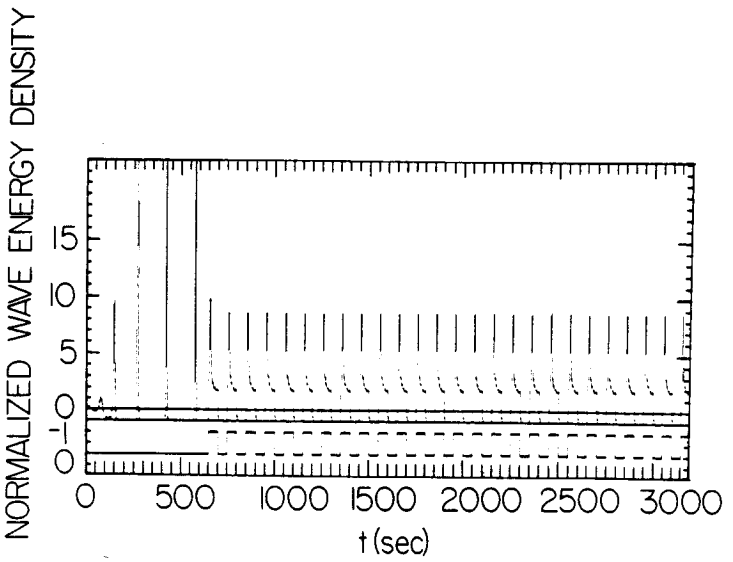

Fig. 5. Simulated, mormalized wave energy density with magnetosphere-ionosphere coupling. A VLF source is turned on at t = 650s.

The maximum ionospheric effect occurs after the wave spike maximum. Our physical interpretation of Figure 4 is as follows. A spike in the wave energy density causes a depletion of electrons trapped in the belts to levels well below the Kennel-Petschek limit. The subsequent drop of precipitating electron flux allows the ionospheric conductivity to decrease. Thus, VLF waves are less strongly reflected back into the magnetosphere. This effectively raises the Kennel-Petschek limit as higher particle fluxes are necessary to offset increased ionospheric VLF absorbtion. In the presence of equatorial sources of particles, the similations show flux levels building to 1.15 times the Kennel-Petschek limit. The enhanced fluxes in the magnetosphere, even with weak pitch angle diffusion, allows the ionospheric conductivity to rise, eventually leading to another masing spike.

Figure (5) shows the effect of an external VLF signal. The first few spikes result from the masing effect of the ionosphere due to particle precipitation. At t = 650 seconds a VLF square wave source is turned on with a 50 second duration. The spikes now are modulated at the driving frequency at a reduced amplitude. The amplitude is reduced since the fluxes are more frequently dumped with the VLF signal present than in its absence.

Iversen et al. (1984) using simultaneous ground and satellite measurements, have recently observed the modulation of precipitating electrons at pulsation frequencies. In terms of our simulations these would be close to the situation shown in Figure 4 in which natural masing occurs in a flux tube. The observed frequencies are consistent with those expected from the linear theory. Detailed comparison with experimental data necessitates knowing the efficiency with which VLF waves reach the ionosphere.

IV Conclusion

Although the work presented in this paper is still in a very preliminary stage of development it appears that significant space effects can be produced by the injection of intense electromagnetic waves into ionospheric plasmas. In the coming months we expect that as calculations mature we will grow in the ability to translate mathematical representation into physical understanding. If the results of our analyses live up to early promise then a series of ground-based wave emission experiments will be developed to measure injection effects in space. The upcoming ECHO-7 experiment presents a well instrumented target of opportunity for electron acceleration experiments with the HIPAS system. After the launch of the CRRES satellite it will be possible to make simultaneous in situ measurements of wave and particle fluxes in artificially excited Alfven Masers. Looking forward to the 1990's it appears that the WISP experiment planned for the Space Station will make an ideal source for both electron acceleration and radiation belt depletion experiments. Recently a Soviet experiment measured electrons accelerated to kilovolt energies using a low power telemetry system (Babaev et al., 1983). Just image that what could be done with the specifically designed, high power WISP!

Bibliography

Babaev, A.P., S.B. Lyakhov, G.G. Managadze, A.A. Martinson and P.P. Timofeev, Plasma particle acceleration due to emission of ground-based and onboard transmitters, in Active Experiments in Space, ESA SP-195 61-65, 1983.

Imhof, W.L., J.B. Reagan, H.D. Voss, E.E. Gaines, D.W. Datlowe, J. Mobilia, R.A. Helliwell, U.S. Inan, J. Katsufrakis, and R.G. Joiner, Direct observation of radiation belt electrons precipitated by the controlled injection of VLF signals from a ground based transmitter, Geophys. Res. Lett., 4, 361 - 364, 1983.

Imhof, W.L., H.D. Voss, J.B. Reagan, D.W. Datlowe and D.S. Evans, Relativistic electron and energetic ion precipitation spikes near the plasmapause, J. Geophys. Res., 91, 3077 - 3088, 1986.

Inan, U.S., T.F. Bell and H. C. Chang, Particle precipitation induced by short duration VLF waves in the magnetosphere, J. Geophys. Res., 87, 6243 - 6264, 1982.

Iversen, I.B., L.P. Block, K. Bronstad, R. Grad, G. Haerendel, H. Junginger, A Korth, G. Kremser M. Madsen, J. Niskanen, W. Riedler, P. Tanskanen, K.M. Torkar, and S. Ullaland, Simultaneous observations of a pulsation event from the ground with balloons and with a geostationary satellite on August 12, 1978, J. Geophys. Res., 89, 6775 - 6785, 1984.

Katsouleas, T., and J.M. Dawson, Unlimited electron acceleration in laser driven plasma waves, Phys. Rev. Lett., 51, 392 - 395, 1983.

Kennel, C.F., and H.E. Petschek, Limit on stably trapped particle fluxes, J. Geophys. Res., 71, 1 - 28, 1966.

Menyuk, C.R., A.T. Drobot, K. Papadopoulos and H. Karimabadi, Stochastic electron acceleration in obliquely propagating electromagnetic waves, SAIC Preprint, 1986

Roberts, C.S., and S.J. Buchsbaum, Motion of a charged particle in a constant magnetic field and a transverse electromagnetic field, Phys. Rev., 135, A381, 1964.

Schulz, M., Particle saturation of the outer zone: a nonlinear model, Astrophys. and Space Sci., 29, 232 - 242, 1974.

Trakhtengerts, V.Yu., Alfven masers, in Active Experiments in Space, ESA SP-195, 67 - 74, 1983.

Wong, A.Y., J. Santoru, and G.G. Sivjee, Active stimulation of the auroral plasma, J. Geophys. Res., 86, 7718 - 7732, 1981.